How to cite: *Angew. Chem. Int. Ed.* **2021**, *60*, 8380–8384
International Edition: doi.org/10.1002/anie.202100349
German Edition: doi.org/10.1002/ange.202100349

Rotaxanes | Hot Paper

Interplay between a Foldamer Helix and a Macrocycle in a Foldarotaxane Architecture

Maxime Gauthier[+], Victor Koehler[+], Caroline Clavel, Brice Kauffmann, Ivan Huc, Yann Ferrand, and Frédéric Coutrot**

Abstract: *The design and synthesis of a novel rotaxane/foldaxane hybrid architecture is reported. The winding of an aromatic oligoamide helix host around a dumbbell-shaped thread-like guest, or axle, already surrounded by a macrocycle was evidenced by NMR spectroscopy and X-ray crystallography. The process proved to depend on the position of the macrocycle along the axle and the associated steric hindrance. The macrocycle thus behaves as a switchable shield that modulates the affinity of the helix for the axle. Reciprocally, the foldamer helix acts as a supramolecular auxiliary that compartmentalizes the axle. In some cases, the macrocycle is forced to move along the axle to allow the foldamer to reach its best recognition site.*

During the past decades, interest for mechanically interlocked molecules has continued unabated because their singular topologies give rise to unique physical and chemical properties. [2]Rotaxanes consist of an end-capped molecular axle threaded into a macrocycle (Figure 1 a). The two stoppering extremities of the axle prevent dethreading, and thus create a mechanical bond that stabilizes the assembly.[1] Rotaxanes' popularity stems in part from their distinct chemical reactivity with respect to their free non-interlaced components.[2] Rotaxanes also enable the implementation of controlled translating motions of the macrocycle along the encircled axle.[3] Within these so-called "molecular shuttles", motion may be triggered by external stimuli, such as solvent effect,[4] variation of temperature,[5] photo-irradiation,[6] molecular recognition[7] or the chemical modifications of an interaction site at the surrounding macrocycle or at the axle. Here, we introduce an alternative approach whereby the position of a threaded macrocycle is controlled by a supramolecular auxiliary, namely a foldamer helix reversibly wound around the same axle.

We have previously described that one or several aromatic foldamer single or double helices may bind to complementary alkyl-carbamate thread-like guests to form pseudo-rotaxane architectures named foldaxanes (Figure 1 b).[8] Such constructs have allowed for the design of molecular pistons in which the foldamer could slide between two regions of the thread.[9] Foldaxanes may form by threading a guest devoid of stoppers,[10] or by winding of the helix around a dumbbell-shaped guest.[9] We thus devised that a foldaxane may form when the axle is already encircled by a macrocycle to produce a three component hybrid assembly (Figure 1 c). In the following, we demonstrate the formation of such "foldarotaxanes".[11] We show that the presence and localization of the macrocycle modulates the association between the helix and the axle. Reciprocally, we highlight the use of the foldamer as a supramolecular auxiliary to compartmentalize[3g,12] the macrocycle around a region of the thread for which it may have a lesser affinity.

The axle of our first foldarotaxane target **1⊃2-HPF$_6$** (Figure 1 f) possesses recognition groups for both a macrocycle and a foldamer single helix. An ammonium moiety directed the synthesis of the interlocked rotaxane through hydrogen bonding to the oxygen atoms of a dibenzo-24-crown-8 macrocycle (DB24C8).[13] The ammonium also behaved as a pH-responsive binding station for the DB24C8 in the final structure. In addition, the axle comprises two carbamate moieties that bind to the 2,6-pyridinedicarboxamide pinchers located at both ends of aromatic foldamer helix **1** (Figure 1 d).[9] Noteworthy, a spacer of a sufficient length between the ammonium and the nearest carbamate was introduced, to prevent that the DB24C8 encircling the ammonium hinders binding of the foldamer helix to the carbamates. Within that spacer, an amide moiety may serve as a secondary binding station for DB24C8:[14] it does not outcompete the ammonium and plays a role only in deprotonated **2** or *N*-carbamoylated **2-Boc** that were subsequently investigated.

Foldarotaxanes were formed via the winding of **1** around the axle of various [2]rotaxanes. The first targeted rotaxane **2-HPF$_6$** was synthesized through a straightforward, ester

[*] M. Gauthier[+,++], Dr. C. Clavel, Dr. F. Coutrot
Supramolecular Machines and ARchitectures Team, Institut des Biomolécules Max Mousseron (IBMM) UMR 5247 CNRS; Université de Montpellier; ENSCM, case courrier 1706, Bâtiment Chimie (17), 3ème étage, Faculté des Sciences
Place Eugène Bataillon, 34095 Montpellier cedex 5 (France)
E-mail: frederic.coutrot@umontpellier.fr
Homepage: http://www.glycorotaxane.fr
V. Koehler[+,++], Dr. Y. Ferrand
Institut de Chimie et Biologie des Membranes et Nano-objets CBMN (UMR5248), Université de Bordeaux, CNRS, IPB
2 rue Robert Escarpit, 33600 Pessac (France)
E-mail: y.ferrand@iecb.u-bordeaux.fr
Dr. B. Kauffmann
Université de Bordeaux, CNRS, INSERM, UMS3033, IECB
2 rue Robert Escarpit, 33600 Pessac (France)
Prof. I. Huc
Department of Pharmacy and Center for Integrated Protein Science
Ludwig-Maximilians-Universität
Butenandtstr. 5–13, 81377 München (Germany)
[+] These authors contributed equally to this work.
[++] Co-first authors
Supporting information and the ORCID identification number(s) for the author(s) of this article can be found under: https://doi.org/10.1002/anie.202100349.

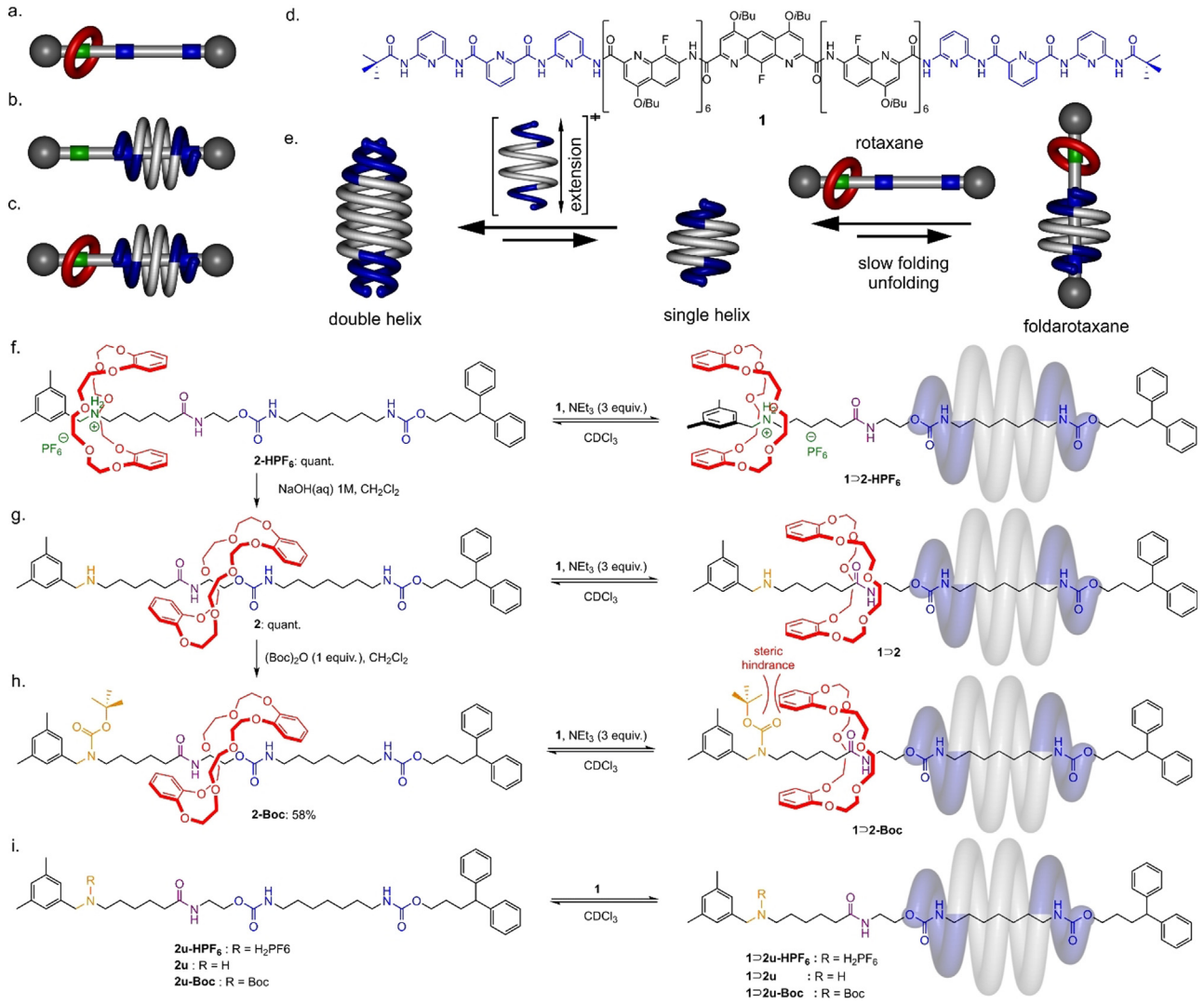

Figure 1. Representation of: a) a rotaxane; b) a foldaxane; c) a foldarotaxane. Templating groups for the macrocycle and the helix are shown in green and blue, respectively. d) Formula of **1** with the same color code as in the helix representation. e) Representation of the equilibria between a double helix and a single helix followed by its winding around a rotaxane leading to the formation of a foldarotaxane. f–i) Preparation of foldarotaxanes **1⊃2-HPF$_6$**, **1⊃2** and **1⊃2-Boc** and of foldaxanes **1⊃2u-HPF$_6$**, **1⊃2u** and **1⊃2u-Boc**.

aminolysis-based, post-interlocking elongation of the encircled axle that preserves the mechanical bond (Schemes S2, S3).[15] As evidenced by ^{1}H and ^{19}F NMR (Figures 2a–d and S9, S10), the corresponding host-guest complex **1⊃2-HPF$_6$** forms readily at room temperature upon adding **2-HPF$_6$** to a solution of single helix **1**. Yet, complex formation is slow at 298 K and competes with the dimerization of **1** into kinetically stable double helix (**1**)$_2$ (Figures 1e, 2b, 3a and S4). To overcome this issue and reach full complexation, the mixture was heated at 318 K,[16] allowing (**1**)$_2$ to disassemble completely into **1**, and affording **1⊃2-HPF$_6$** as the thermodynamically most stable species (Figure 2d). As with other foldaxanes,[9] the distinct resonances of **1⊃2-HPF$_6$** indicate slow exchange with **1** and (**1**)$_2$ on the NMR time scale. Worthy of note is the splitting of the signals of the entwined helix of **1⊃2-HPF$_6$** as a typical signature of a symmetrical helix bound to a dissymmetrical thread. The integration of the signals of each species at thermodynamic equilibrium allowed to determine the association constant ($K_a = 207\,000$ M^{-1}, Table 1).

Further characterization of foldarotaxane **1⊃2-HPF$_6$** was performed using X-ray crystallography (Figure 3b–e). Single crystals were obtained by the slow diffusion of hexane in a chlorobenzene solution of **1⊃2-HPF$_6$**. The structure validated the initial design, with the DB24C8 positioned on the ammonium group and the foldamer helix on the dicarbamate station. One of the DB24C8 aromatic units stacks on the terminal xylyl stoppers. The thread was found to be kinked with an angle of 86.1° allowing the formation of an intramolecular hydrogen bond between the carbonyl oxygen atom

Table 1: Association constants[a] (K_a) relative to the formation of foldarotaxanes and foldaxanes.

	1⊃2-HPF$_6$	1⊃2	1⊃2-Boc	1⊃2u-HPF$_6$	1⊃2u	1⊃2u-Boc
K_a [10^3 M^{-1}]	207	9.1	3.8	375	397	317

[a] Association constants calculated with: $K_a = ([\text{axle-helix complex}]^2 K_{dim}/([(\mathbf{1})_2][\text{axle}]^2))^{0.5}$ with $K_{dim} = [(\mathbf{1})_2]/[\mathbf{1}]^2$.

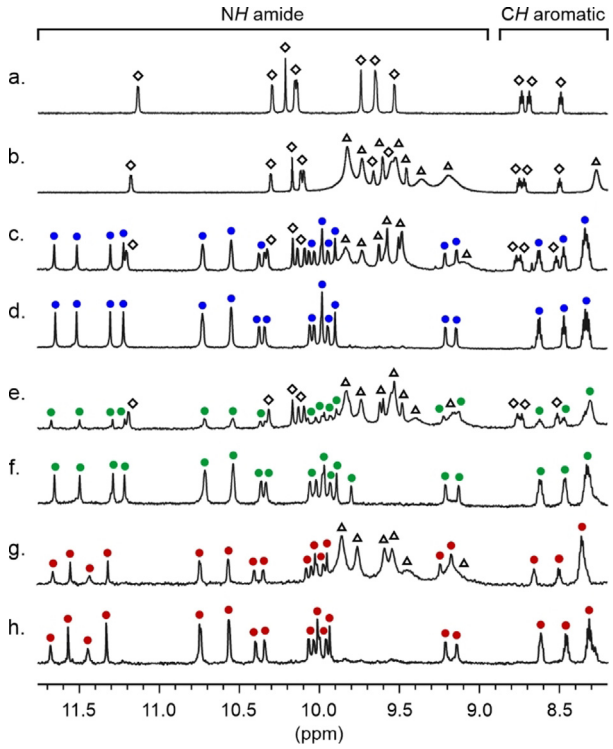

Figure 2. Sections of 700 MHz ^{1}H NMR spectra (298 K in $CDCl_3$ at 0.1 mM of **1**) showing the amide resonances of: a) single helix **1** obtained by precipitation in methanol; b) a mixture of single helix **1** and double helix $(\mathbf{1})_2$. Titration experiments showing the winding of the single helix **1** around protonated rotaxanes: c) 0.5 equiv. of **2-HPF$_6$** and d) 2.5 equiv. of **2-HPF$_6$**; e) 0.5 equiv. of **2** and f) 4 equiv. of **2**; g) 0.5 equiv. of **2-Boc** and h) 7 equiv. of **2-Boc**. Signals of the double helix and the single helix are marked with empty triangles and empty diamonds, respectively. Signals of the protonated foldarotaxane **1⊃2-HPF$_6$**, the deprotonated foldarotaxane **1⊃2** and carbamoylated foldarotaxane **1⊃2-Boc** are marked with blue, green and red circles, respectively.

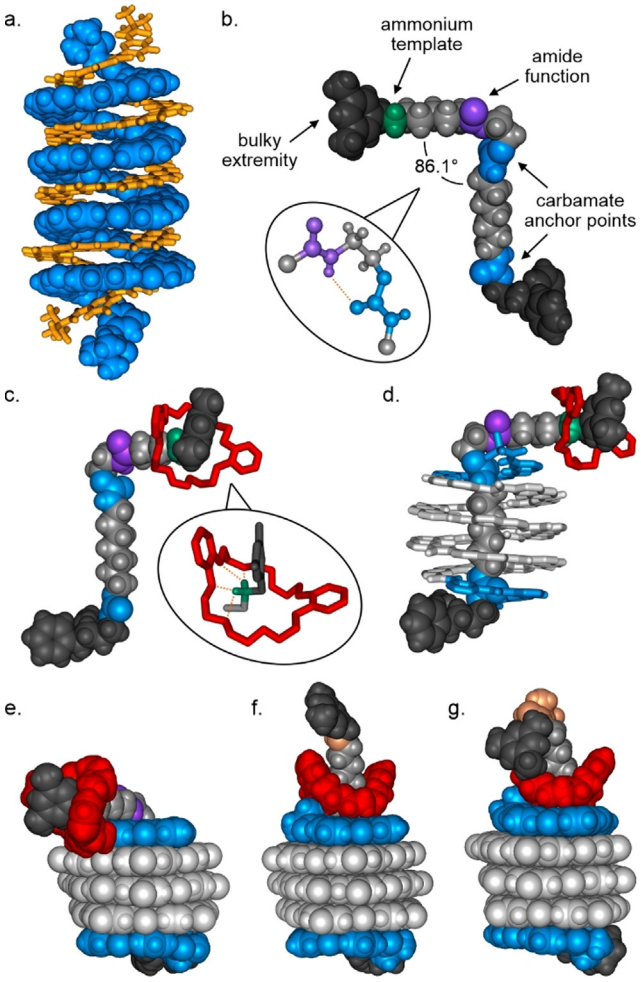

Figure 3. Structures in the solid state analyzed by X-ray crystallography of: a) the double helix $(\mathbf{1})_2$ and b–e) the protonated foldarotaxane **1⊃2-HPF$_6$**. In (a) $(\mathbf{1})_2$ is shown with one strand in an orange tube representation whereas the other strand is shown in a blue CPK representation. b) Structure of the dumbbell-shaped guest equipped with functional groups to bind to the DB24C8 macrocycle and single helix **1**. Enlargement of the dumbbell-shaped guest showing a kink due to a hydrogen bond between the amide and the carbamate functions of the thread. c) The rotaxane **2-HPF$_6$** as it exists in the structure of **1⊃2-HPF$_6$** and an enlargement highlighting the binding mode between DB24C8 and its ammonium template. d,e) The protonated foldarotaxane **1⊃2-HPF$_6$**. Side views of the energy-minimized molecular models (using Merck Molecular Force Field static, MMFFs) of: f) **1⊃2** and g) **1⊃2-Boc**. In (b), (c) and (d), the helix and the macrocycle are shown as a tube representation whereas the dumbbell-shaped guest is shown as a CPK representation. In (e), (f), and (g), all the components are shown as space-filling representations. The functional groups are color coded as in Figure 1. Hydrogen bonds are represented with orange dashed lines. Helix side chains (O*i*Bu groups) and included solvent molecules have been removed for clarity.

of a carbamate and the N*H* of the neighboring amide group (Figure 3b).

We next investigated the influence of the macrocycle position along the axle on the helix association and whether potential steric conflicts or competition for the same binding station would occur. Deprotonated **2** and *N*-carbamoylated **2-Boc** [2]rotaxanes were considered for the study. For both interlocked architectures, deprotonation or deprotonation-carbamoylation of the ammonium station resulted in the shuttling of the DB24C8 toward both the amide and the neighboring carbamate moiety, with which it interacts through hydrogen bonds (Figure 1g,h, see also Figures S6–8 for NMR evidence). Adding [2]rotaxanes **2** or **2-Boc** to single helix **1** led to the formation of foldarotaxanes **1⊃2** and **1⊃2-Boc**, respectively (Figure 2e–h). K_a values proved to be significantly reduced as compared to that measured for **1⊃2-HPF$_6$**, highlighting a protecting effect of DB24C8 with respect to helix binding.[17] Since deprotonation and *t*-butyl-carbamoylation are both invertible, these changes are in principle switchable.

Specifically, **1** has a 23-fold lower affinity for **2** than for **2-HPF$_6$** (Table 1). This lesser affinity may be partly assigned to the DB24C8 that competes with the helix to hydrogen bond to the amide and the carbamate groups. Nevertheless, binding remains high and the formation of **1⊃2** remains quantitative at submicromolar concentrations (Figure 2f), which displaces the macrocycle from its initial thermodynamically more favorable carbamate-amide station (Figure 1g, left). The helix can thus be viewed as a supramolecular auxiliary that

traps the DB24C8 within a compartment of the axle for which its affinity is lower.

Quantitative foldarotaxane formation also occurs with **2-Boc** (Figure 2h). In this case, the Boc group further reduces the space available to accommodate the DB24C8 when it is displaced by the helix from the amide-carbamate station (Figure 1h). Furthermore, upon winding of the helix, the carbamoylated amine of **2-Boc** cannot assist the displacement of the DB24C8 through electronic attraction, on contrary to **2** that possesses a free amine as a very weak site of interaction for the DB24C8.[18] It follows that helix binding is further reduced ($K_a = 3800\ M^{-1}$, Table 1). For comparison, association constants were also determined for the foldaxane analogues, **1⊃2u-HPF$_6$**, **1⊃2u** and **1⊃2u-Boc** (Figure 1i). All the foldaxanes were found to be slightly more stable than **1⊃2-HPF$_6$** (K_a values from 317000 to 397000 M^{-1}), corroborating the fact that the DB24C8 does not significantly disturb the wrapping of the helix around the dicarbamate region of the axle when it sits around the ammonium station.[19] Notwithstanding such effects, binding of **1** to **2u** and **2u-Boc** is stronger than to **2** and **2-Boc**, respectively, confirming the partial protective shielding effect of the DB24C8 against the helix both in deprotonated and *N*-carbamoylated states. Energy-minimized molecular models of **1⊃2** and **1⊃2-Boc** (Figures 3f,g, S22, S23) reveal a bulk interface between the helix and the macrocycle, which may be responsible for some steric hindrance. In the case of **1⊃2-Boc** the Boc protective group of the secondary amine requires the macrocycle to be pressed onto the helix.

In conclusion, we have reported the design of several foldarotaxanes through the winding of a helix around the encircled thread of [2]rotaxanes. The recognition between the helix and rotaxane's thread is reminiscent of an allosteric system.[18a] Chemical reactions at one end of the encircled thread of [2]rotaxanes trigger *co*-conformational changes through the shuttling of the macrocycle, therefore inducing an alteration of the recognition of the [2]rotaxane for the helix at the other end. Through its controlled and switchable position, the macrocycle may thus act as a tunable moderator of the affinity of the encircled axle for the helix. Conversely, the helix acts as a supramolecular auxiliary to compartmentalize the rotaxane molecular shuttle through the induced translation of the macrocycle out from its best recognition site. These results pave the way to the design of foldarotaxane molecular machines that might operate through interdependent motions of both helix and macrocycle. Such studies are currently in progress in our laboratories and will be reported in due course.

Acknowledgements

We thank the "Agence Nationale de la Recherche" for funding the project ANR-17-CE07-0014-01 and the France-Germany International Research Project "Foldamers Structures and Functions" (IRP FoldSFun). This work benefited from the facilities and expertise of the Biophysical and Structural Chemistry platform at IECB, CNRS UMS3033, INSERMUS001, and Bordeaux University, France.

Conflict of interest

The authors declare no conflict of interest.

Keywords: crystallography · foldamers · molecular motion · rotaxanes

[1] C. J. Bruns, J. F. Stoddart, *The nature of the mechanical bond: From Molecules to Machines*, Wiley, Hoboken, **2016**.

[2] a) E. A. Neal, S. M. Goldup, *Chem. Commun.* **2014**, *50*, 5128–5142; b) P. Waelès, M. Gauthier, F. Coutrot, *Angew. Chem. Int. Ed.* **2021**, https://doi.org/10.1002/anie.202007496; *Angew. Chem.* **2021**, https://doi.org/10.1002/ange.202007496; c) J. Gassensmith, J. M. Baumes, B. D. Smith, *Chem. Commun.* **2009**, 6329–6338; d) M. J. Frampton, H. L. Anderson, *Angew. Chem. Int. Ed.* **2007**, *46*, 1028–1064; *Angew. Chem.* **2007**, *119*, 1046–1083; e) A. Martinez-Cuezva, C. Lopez-Leonardo, M. Alajarin, J. Berna, *Synlett* **2019**, *30*, 893–902; f) F. Modicom, E. M. G. Jamieson, E. Rochette, S. M. Goldup, *Angew. Chem. Int. Ed.* **2019**, *58*, 3875–3879; *Angew. Chem.* **2019**, *131*, 3915–3919.

[3] a) H. Tian, Q.-C. Wang, *Chem. Soc. Rev.* **2006**, *35*, 361–374; b) S. Silvi, M. Venturi, A. Credi, *J. Mater. Chem.* **2009**, *19*, 2279–2294; c) S. Erbas-Cakmak, D. A. Leigh, C. T. McTernan, A. L. Nussbaumer, *Chem. Rev.* **2015**, *115*, 10081–10206; d) F. Coutrot, *ChemistryOpen* **2015**, *4*, 556–576; e) H.-Y. Zhou, Y. Han, C.-F. Chen, *Mater. Chem. Front.* **2020**, *4*, 12–28; f) S. Kassem, T. van Leeuwen, A. S. Lubbe, M. R. Wilson, B. L. Feringa, D. A. Leigh, *Chem. Soc. Rev.* **2017**, *46*, 2592–2621; g) E. R. Kay, D. A. Leigh, F. Zerbetto, *Angew. Chem. Int. Ed.* **2007**, *46*, 72–191; *Angew. Chem.* **2007**, *119*, 72–196.

[4] a) D. A. Leigh, M. A. F. Morales, E. M. Pérez, J. K. Y. Wong, C. G. Saiz, A. M. Z. Slawin, A. J. Carmichael, D. M. Haddleton, A. M. Brouwer, W. J. Buma, G. W. H. Wurpel, S. León, F. Zerbetto, *Angew. Chem. Int. Ed.* **2005**, *44*, 3062–3067; *Angew. Chem.* **2005**, *117*, 3122–3127; b) C. Romuald, A. Ardá, C. Clavel, J. Jiménez-Barbero, F. Coutrot, *Chem. Sci.* **2012**, *3*, 1851–1857; c) H. Tian, R. Li, P.-H. Lin, K. Meguellati, *New J. Chem.* **2020**, *44*, 10628.

[5] a) E. Busseron, C. Romuald, F. Coutrot, *Chem. Eur. J.* **2010**, *16*, 10062–10073; b) D. Inamori, H. Masai, T. Tamaki, J. Terao, *Chem. Eur. J.* **2020**, *26*, 3385–3389.

[6] a) A. Altieri, G. Bottari, F. Dehez, D. A. Leigh, J. K. Y. Wong, F. Zerbetto, *Angew. Chem. Int. Ed.* **2003**, *42*, 2296–2300; *Angew. Chem.* **2003**, *115*, 2398–2402; b) J. J. Yu, L. Y. Zhao, Z. T. Shi, Q. Zhang, G. London, W. J. Liang, C. Gao, M. M. Li, X. M. Cao, H. Tian, B. L. Feringa, D. H. Qu, *J. Org. Chem.* **2019**, *84*, 5790–5802.

[7] A. Martinez-Cuezva, J. Berna, R.-A. Orenes, A. Pastor, M. Alajarin, *Angew. Chem. Int. Ed.* **2014**, *53*, 6762–6767; *Angew. Chem.* **2014**, *126*, 6880–6885.

[8] Y. Ferrand, I. Huc, *Acc. Chem. Res.* **2018**, *51*, 970–977.

[9] a) Q. Gan, Y. Ferrand, C. Bao, B. Kauffmann, A. Grélard, H. Jiang, I. Huc, *Science* **2011**, *331*, 1172–1175; b) Y. Ferrand, Q. Gan, B. Kauffmann, H. Jiang, I. Huc, *Angew. Chem. Int. Ed.* **2011**, *50*, 7572–7575; *Angew. Chem.* **2011**, *123*, 7714–7717; c) S. A. Denisov, Q. Gan, X. Wang, L. Scarpantonio, Y. Ferrand, B. Kauffmann, G. Jonusauskas, I. Huc, N. D. McClenaghan, *Angew. Chem. Int. Ed.* **2016**, *55*, 1328–1333; *Angew. Chem.* **2016**, *128*, 1350–1355; d) Q. Gan, X. Wang, B. Kauffmann, F. Rosu, Y. Ferrand, I. Huc, *Nat. Nanotechnol.* **2017**, *12*, 447–454.

[10] X. Wang, B. Wicher, Y. Ferrand, I. Huc, *J. Am. Chem. Soc.* **2017**, *139*, 9350–9358.

[11] We define here a foldarotaxane as the combination of a foldaxane and a rotaxane around the same axle. Foldamers and rotaxanes have previously been combined in other ways, for example when a foldamer is an integral part of the axle of

a rotaxane, see for example: a) K.-D. Zhang, X. Zhao, G.-T. Wang, Y. Liu, Y. Zhang, H.-J. Lu, X.-K. Jiang, Z.-T. Li, *Angew. Chem. Int. Ed.* **2011**, *50*, 9866 – 9870; *Angew. Chem.* **2011**, *123*, 10040 – 10044; b) W.-K. Wang, Z.-Y. Xu, Y.-C. Zhang, H. Wang, D.-W. Zhang, Y. Liu, Z.-T. Li, *Chem. Commun.* **2016**, *52*, 7490 – 7493; c) D. A. Leigh, L. Pirvu, F. Schaufelberger, D. J. Tetlow, L. Zhang, *Angew. Chem. Int. Ed.* **2018**, *57*, 10484 – 10488; *Angew. Chem.* **2018**, *130*, 10644 – 10648; d) A. Moretto, I. Menegazzo, M. Crisma, E. J. Shotton, H. Nowell, S. Mammi, C. Toniolo, *Angew. Chem. Int. Ed.* **2009**, *48*, 8986 – 8989; *Angew. Chem.* **2009**, *121*, 9148 – 9151.

[12] For background on the concept of compartmentalization, see a) J. S. Hannam, S. M. Lacy, D. A. Leigh, C. G. Saiz, A. M. Z. Slawin, S. G. Stitchell, *Angew. Chem. Int. Ed.* **2004**, *43*, 3260 – 3264; *Angew. Chem.* **2004**, *116*, 3322 – 3326; b) M. N. Chatterjee, E. R. Kay, D. A. Leigh, *J. Am. Chem. Soc.* **2006**, *128*, 4058 – 4073; c) V. Serreli, C.-F. Lee, E. R. Kay, D. A. Leigh, *Nature* **2007**, *445*, 523 – 527; d) E. R. Kay, D. A. Leigh, *Pure Appl. Chem.* **2008**, *80*, 17 – 29; e) M. Alvarez-Pérez, S. M. Goldup, D. A. Leigh, A. M. Z. Slawin, *J. Am. Chem. Soc.* **2008**, *130*, 1836 – 1838; f) A. Carlone, S. M. Goldup, N. Lebrasseur, D. A. Leigh, A. Wilson, *J. Am. Chem. Soc.* **2012**, *134*, 8321 – 8323; g) E. Busseron, F. Coutrot, *J. Org. Chem.* **2013**, *78*, 4099 – 4106; h) W.-K. Wang, Z.-Y. Xu, Y.-C. Zhang, H. Wang, D.-W. Zhang, Y. Liu, Z.-T. Li, *Chem. Commun.* **2016**, *52*, 7490 – 7493; i) Y. Mochizuki, K. Ikeyatsu, Y. Mutoh, S. Hosoya, S. Saito, *Org. Lett.* **2017**, *19*, 4347 – 4350.

[13] A. G. Kolchinski, D. H. Busch, N. W. Alcock, *J. Chem. Soc. Chem. Commun.* **1995**, 1289 – 1291.

[14] B. Riss-Yaw, J. Morin, C. Clavel, F. Coutrot, *Molecules* **2017**, *22*, 2017.

[15] a) T. Legigan, B. Riss-Yaw, C. Clavel, F. Coutrot, *Chem. Eur. J.* **2016**, *22*, 8835 – 8847; b) B. Riss-Yaw, T. X. Métro, F. Lamaty, F. Coutrot, *RSC Adv.* **2019**, *9*, 21587 – 21590.

[16] This was achieved in the presence of Et_3N (3 equiv.) to prevent any adverse acidity from $CDCl_3$ decomposition, which may cause the protonation of the pyridyl units of the helix, hence its unfolding. Note that this amount of Et_3N does not deprotonate the ammonium moiety of the [2]rotaxane which is stabilized upon interacting with DB24C8. For a reference, see: N. Kihara, Y. Tachibana, H. Kawasaki, T. Takata, *Chem. Lett.* **2000**, *29*, 506 – 507.

[17] For other examples related to the protection of functionalities on a thread by a macrocycle, see: a) T. Oku, Y. Furusho, T. Takata, *Org. Lett.* **2003**, *5*, 4923 – 4925; b) A. H. Parham, B. Windisch, F. Vögtle, *Eur. J. Org. Chem.* **1999**, 1233 – 1238; c) D. A. Leigh, E. M. Pérez, *Chem. Commun.* **2004**, 2262 – 2263; d) A. Mateo-Alonso, P. Brough, M. Prato, *Chem. Commun.* **2007**, 1412 – 1414; e) F. Scarel, G. Valenti, S. Gaikwad, M. Marcaccio, F. Paolucci, A. Mateo-Alonso, *Chem. Eur. J.* **2012**, *18*, 14063 – 14068; f) D. M. D'Souza, D. A. Leigh, L. Mottier, K. M. Mullen, F. Paolucci, S. J. Teat, S. Zhang, *J. Am. Chem. Soc.* **2010**, *132*, 9465 – 9470; g) M. Gauthier, F. Coutrot, *Eur. J. Org. Chem.* **2019**, *21*, 3391 – 3395; h) M. Franz, J. A. Januszewski, D. Wendinger, C. Neiss, L. D. Movsisyan, F. Hampel, H. L. Anderson, A. Görling, R. R. Tykwinski, *Angew. Chem. Int. Ed.* **2015**, *54*, 6645 – 6649; *Angew. Chem.* **2015**, *127*, 6746 – 6750; i) A. Fernandes, A. Viterisi, F. Coutrot, S. Potok, D. A. Leigh, V. Aucagne, S. Papot, *Angew. Chem. Int. Ed.* **2009**, *48*, 6443 – 6447; *Angew. Chem.* **2009**, *121*, 6565 – 6569; j) N. Kihara, S. Motoda, T. Yokozawa, T. Takata, *Org. Lett.* **2005**, *7*, 1199 – 1202.

[18] Similarly, it has been shown that the reactivity of a function, when in interaction with an encircling DB24C8, may depend on the proximity of another site of recognition, see: a) G. Ragazzona, C. Schäfera, P. Franchia, S. Silvia, B. Colasson, M. Lucarini, A. Credi, *Proc. Natl. Acad. Sci. USA* **2018**, *115*, 9385 – 9390; b) C. Romuald, E. Busseron, F. Coutrot, *J. Org. Chem.* **2010**, *75*, 6516 – 6531; c) G. Ragazzon, A. Credi, B. Colasson, *Chem. Eur. J.* **2017**, *23*, 2149 – 2156.

[19] In order to make a comparison, the association constant in chloroform at 293 K between a similar dialkylammonium and the DB24C8 is about 500 M^{-1}. It is much lower with amide and even lower with carbamate.

Manuscript received: January 8, 2021
Accepted manuscript online: January 21, 2021
Version of record online: March 10, 2021

